

Influence of Modeling Methods on the Estimation of the Nonlinear Noise Statistics Considering Joint PMD and Kerr Effects in Fiber Transmission Systems

Sina Fazel, Djalal-Falih Bendimerad, Nicola Rossi, Petros Ramantanis and Yann Frignac

Abstract—In the recent context of Software Defined Optical Network, the fast and accurate Quality of Transmission (QoT) estimation of the transmission link is essential. Gaussian Noise models are shown to yield a fast estimation of the average QoT derived from deterministic system parameters, but do not capture the QoT variability. In order to assess numerically the stochastic joint effect of Polarization Mode Dispersion (PMD) and Kerr nonlinearities, system designers generally use the Split Step Fourier Method (SSFM) based on Manakov-PMD equation neglecting the nonlinear-PMD term which is faster than using Coupled NonLinear Schrödinger Equation (CNLSE) and enough accurate for fiber with short birefringence correlation length (around less than 10m). In this work, we present insights of the way to tune the parameters of this Manakov-PMD method and its limitation when seeking an accurate estimation of the Non-Linear Interference (NLI) noise statistical distribution for all fibers potentially installed in the current optical network. In particular we compare this Manakov-PMD method results with respect to the one obtained by CNLSE while varying the fiber birefringence correlation length, PMD coefficient and the fiber type. Our results highlight a potential discrepancy of 0.5 dB in the estimation of the Q^2 factor in one span Polarization Division Multiplexed Quadrature Phase Shift Keying (PDM-QPSK) transmission with optimal launch power per channel and yield guidelines to choose the most suitable numerical estimation method.

Index Terms—(060.0060) Fiber optics and optical communications; (060.2330) Fiber optics communications.

I. INTRODUCTION

THE concept of Software Defined Networks (SDNs) has been recently proposed to provide the necessary flexibility and reliability to handle the increasing network traffic demand [1]. In this context, a fast tool that could estimate the QoT is of particular interest. The QoT estimation is strongly motivated by network providers as a wise choice of the system margins that can ensure the network reliability

with no additional cost brought by excessive opto-electronic regeneration transponders. In the fiber optic communications domain, recent work on such analytical or semi-analytical tools has been shown to provide promising solutions for that purpose, with the most prominent such model being the Gaussian Noise (GN) model [2].

However, it has been recently shown that the Bit Error Rate (BER) (or Q^2 factor) can be more accurately described by a random variable rather than a constant value due to the stochastic nature of the NLI, which highlights variability in the GN model performance estimation, particularly in Dispersion Management (DM) transmission systems [3], [4]. One among several phenomena that can randomly influence the QoT is PMD [5]–[7]. Although recent advances in Digital Signal Processing (DSP) embedded in the coherent receivers can overcome the impairments induced by PMD itself, the interplay of PMD and Kerr nonlinearity causes stochastic variations of transmission performance [8]–[12]. To assess PMD and Kerr nonlinearity interaction, traditionally the well-known SSFM has been used to numerically estimate the evolution of signals along the propagation based on the CNLSE [13], [14]. The SSFM inherently requires a large amount of Fast Fourier Transform (FFT) steps to fairly emulate both chromatic dispersion and Kerr nonlinearity. In such circumstances, PMD adds more processing requirements due to an additional fiber splitting step and a massive set of random draws of fiber birefringence concatenations to properly investigate the whole probability distributions of the possible Differential Group Delay (DGD) between signal polarization tributaries [15], [16]. Thus simulating transmission systems involving PMD and Kerr nonlinearity implies a large amount of time-consuming computations. Manakov-PMD method is offering an efficient way to reduce the computational complexity by emulating only the averaged Kerr nonlinear effects through the polarization states, assuming that the correlation length ($L_{corr.}$) of the fiber birefringence is much lower than the Kerr nonlinear length (L_{Kerr}) [17]. Authors in [17] have made the theoretical basis deriving from the CNLSE an equivalent equation called Manakov-PMD equation and have shown that its nonlinear-PMD term can be fairly neglected by a numerical simulation in 1997 using legacy 5 Gbits/s NRZ single-channel and single-polarization transmission with computation constraints of the time imposing short sequence lengths and a few fiber random birefringence draws. In this paper we will refer to

S. Fazel was with Department of Physics and Electronics, CNRS SAMOVAR, Télécom SudParis, Institut Polytechnique de Paris when this work was carried out. He is currently with Delft Center of Systems and Control (DCSC), Delft University of Technology, Delft, The Netherlands.

D. Bendimerad was with Department of Physics and Electronics, CNRS SAMOVAR, Télécom SudParis, Institut Polytechnique de Paris when this work was carried out. He is currently with The Optical Communication Technology Lab, Huawei Paris Research Centre, France

N. Rossi was with Nokia Bell Labs when this work was carried out. He is currently with Alcatel Submarine Networks (ASN), 91620 Nozay, France.

P. Ramantanis is with Nokia Bell Labs, 91620 Nozay, France.

Y. Frignac is a Professor at the Department of Physics and Electronics, CNRS SAMOVAR, Télécom SudParis, Institut Polytechnique de Paris, France. e-mail: yann.frignac@telecom-sudparis.eu

the manakov-PMD method as the one describe in [17] while neglecting the nonlinear-PMD term or equivalently the Eq. 68 of [8]. Later, many studies of joint PMD and Kerr nonlinearity have been performed generally tackling very particular system configurations [15], [16]. While the computation of the signal propagation based on Manakov-PMD equation neglecting the nonlinear-PMD term is clearly less time consuming, it should be noticed this can not be blindly applied for all fiber types of the installed network as it may yields to NLI noise estimation error.

In order to help system designers to find the most accurate and fast approach to estimate the QoT variability, here we take profit of recent computational means and the above-mentioned SDN-driven motivation to perform a massive amount of SSFM-based Wavelength Division Multiplexed (WDM) transmission system simulations through both CNLSE and Manakov-PMD method with different fiber correlation lengths and the context of recent Polarization Division Multiplexing coherent transmission systems. Inspired by previous modeling efforts that separate the influence of the number of spans and other system parameters [18]–[20] and in an effort to simplify our system under study, in this paper we assess the power-independent NLI coefficient a_{NL} as a Random Variable (RV) [3] also depending on the fiber random birefringence concatenation after a one-span transmission via either Manakov-PMD or CNLSE methods. The two methods are here specifically compared through the estimation of the average values and standard deviations of a_{NL} . Moreover, in our investigations the PMD is taken into account only through its first order while varying the fiber PMD coefficient and fiber types.

The paper is organized as follows. In section 2 we review the numerical methods for the estimation of transmission quality in presence of PMD and Kerr effect. This section contains SSFM description accounting for PMD and Kerr effect using either CNLSE or Manakov-PMD methods, fundamentals of GN modeling to estimate NLI noise accumulation, our simulation setup and finally NLI noise statistics estimation process. Next in section 3, first we highlight the difference in NLI noise statistics estimation using either CNLSE or Manakov-PMD equation while varying the number of birefringent plate employed to model the PMD effect along the propagation link. Later, we analyze how the results are modified while changing the PMD coefficient and fiber type. In the end, we give insights on choosing the most suitable method depending on the birefringence correlation length of the fiber to be modeled and quantify the estimation error made by using inadequate method.

II. TRANSMISSION SYSTEM PERFORMANCE ESTIMATION IN PRESENCE OF PMD AND KERR NONLINEAR EFFECTS

A. Split Step Fourier Method fiber propagation modeling in presence of PMD and Kerr nonlinearity

Modeling the propagation of dual polarization modulated signals in the fiber generally relies on the simplified CNLSE formalism, shown in Eq. (1), which gives the evolution of the slow varying envelopes $A_x(z, t)$ and $A_y(z, t)$ along the

Fiber type	L_{corr} . [m]	PMD coefficient [ps/\sqrt{km}]
G.652	23	0.05
G.653	10	0.06
G.655	19	0.05

TABLE I

EXAMPLES OF CORRELATION LENGTH L_{corr} . AND PMD COEFFICIENT MEASUREMENTS FROM LITERATURE [28], [30].

propagation distance z assuming only loss, second order chromatic dispersion and Kerr nonlinear effects [14].

$$\begin{cases} \frac{\partial A_x}{\partial z} + \beta_{1x} \frac{\partial A_x}{\partial t} + \frac{i\beta_{2x}}{2} \frac{\partial^2 A_x}{\partial t^2} + \frac{\alpha_x}{2} A_x = i\gamma(|A_x|^2 + \frac{2}{3}|A_y|^2)A_x \\ \frac{\partial A_y}{\partial z} + \beta_{1y} \frac{\partial A_y}{\partial t} + \frac{i\beta_{2y}}{2} \frac{\partial^2 A_y}{\partial t^2} + \frac{\alpha_y}{2} A_y = i\gamma(|A_y|^2 + \frac{2}{3}|A_x|^2)A_y \end{cases} \quad (1)$$

In the equation Eq. (1), all $\beta_n(\omega)$ indicate the n^{th} derivatives of the propagation constant β as a function of ω around the overall signal center angular frequency ω_0 , α indicates the fiber attenuation coefficient and γ is the nonlinear coefficient. Note that the $\beta_{2,x/y}$ and the $\alpha_{x/y}$ are here assumed equal for both polarization components (i.e. Polarization Dependent Loss is neglected). Note that $A_x(z, t)$ and $A_y(z, t)$ do not represent the envelopes of a given channel but the total WDM field envelop of each polarization. Thus equation Eq. (1) includes inherently Four Wave Mixing (FWM) for each polarization state.

The numerical calculation of the CNLSE can be made by the use of SSFM algorithm which successively applies nonlinear and dispersive steps [14], [21]. Optimized SSFM algorithms mainly consider nonlinear step that accumulates a constant amount of additional nonlinear phase ϕ_{NL} [22], [23]. As the signal power is exponentially decreasing along the fiber, the emulated step length is thus increasing. It is worth noting that the accuracy of the SSFM depends on the maximum nonlinear phase ($\phi_{NL,max}$) that can be accumulated in one step [14].

On the other hand, we model the fiber under test as concatenation of birefringent over the previous SSFM fiber steps to model the PMD. This results in a concatenation of successive plates each being with constant birefringence and randomly drawn birefringence axis. The length of fiber within which the birefringence properties can be considered constant is referred to as the correlation length L_{corr} . [24]–[30]. For accurate estimation of the PMD, length of the plates has to be chosen equal to the L_{corr} . of a real fiber. For instance, some previous measurements indicate (see Tab. I) a L_{corr} . from about 10 to 100 meters respectively corresponding to 10 000 to 1000 plates in order to emulate a 100km-long fiber span. For a reasonable time consumption, SSFM simulations based on the CNLSE are generally using a lower number of plates yet with the cost of a loss of accuracy in the calculation (see section III-A).

While the correlation length is much lower than the nonlinear Kerr length ($L_{corr} \ll L_{Kerr}$), the nonlinear effects on signals can be modeled as somehow averaged over polarizations, following the traditional Manakov-PMD equation (see Eq. 2) instead of the CNLSE (derived from Eq. 68 in [8]). We recall as previously explained in the introduction

that the nonlinear-PMD term is neglected as it is described in [8]. This method has the advantage of effectively reducing the simulation computation time [17], [31], [32].

$$\begin{cases} \frac{\partial A_x}{\partial z} + \beta_{1x} \frac{\partial A_x}{\partial t} + \frac{i\beta_{2x}}{2} \frac{\partial^2 A_x}{\partial t^2} + \frac{\alpha_x}{2} A_x = i\gamma \frac{8}{9} (|A_x|^2 + |A_y|^2) A_x \\ \frac{\partial A_y}{\partial z} + \beta_{1y} \frac{\partial A_y}{\partial t} + \frac{i\beta_{2y}}{2} \frac{\partial^2 A_y}{\partial t^2} + \frac{\alpha_y}{2} A_y = i\gamma \frac{8}{9} (|A_y|^2 + |A_x|^2) A_y \end{cases} \quad (2)$$

As the terms $(|A_x|^2)A_x$ and $(|A_y|^2)A_y$ in the CNLSE equation (Eq. (1)) are related to Kerr nonlinearities within each polarization tributary while the terms $(\frac{2}{3}|A_x|^2)A_x$ and $(\frac{2}{3}|A_y|^2)A_y$ are referring to Cross-Polarization nonlinearities, we can observe that the $\frac{8}{9}$ coefficient in the Manakov-PMD equation (Eq. (2)) undermines the weights of intra-tributary nonlinearities of PDM tributaries with respect to the weights of cross polarization nonlinear effects.

B. Introducing Q^2 factor and a_{NL} , nonlinear noise coefficient in Gaussian noise modeling

The BER of systems impacted by Additive White Gaussian Noise (AWGN) has been studied extensively in classical digital communications and simple closed form formulas exist for the BER as a function of the Signal to Noise Ratio (SNR) for various modulation formats. E.g. for Quadrature Phase Shift Keying (QPSK) modulation, the BER is given by the well-known formula [33]

$$BER = \frac{1}{2} \operatorname{erfc} \left(\sqrt{\frac{SNR}{2}} \right) \quad (3)$$

where the SNR is defined as

$$SNR = \frac{P}{P_N} \quad (4)$$

with P the signal power and P_N the total noise power or noise variance.

In optical 10Gbps On Off Keying (OOK) systems, supposing Gaussian statistics for the two symbols, the BER could be given as a function of the Q factor using the formula [34]

$$BER = \frac{1}{2} \operatorname{erfc} \left(\frac{Q}{\sqrt{2}} \right) \quad (5)$$

Even though 10Gbps OOK systems have almost entirely given their place to coherent 100Gbps systems, in optical communication systems it is customary to convert BER (e.g. obtained by lab measurements by Monte-Carlo error counting) into an equivalent Q_{BER} (i.e. Q factor obtained from BER) by inverting eq. 5

$$Q_{BER} = \sqrt{2} \operatorname{erfc}^{-1}(2BER) \quad (6)$$

As it can be seen from Eqs. 3 and 6, for an optical coherent system with QPSK modulation and Gaussian noise statistics, we expect $Q_{BER}^2 = SNR$.

As shown in [35], [36], [18], the distortion due to the nonlinear Kerr effect in coherent Dispersion Unmanaged (DU) systems can be treated as an additive AWGN term, i.e. assuming no correlation between NLI "noise" and Amplified

Spontaneous Emission (ASE) noise, the SNR at the receiver can be written as [19]

$$SNR = \frac{P_s}{P_{ASE} + P_{NL} + P_{TRX}} \quad (7)$$

where P is the received signal power, P_{ASE} is the noise variance added by the amplifiers, P_{TRX} accounts for the distortion due to transponder imperfections and P_{NL} is the NLI "noise" variance. In the same (GN model) context, the NLI "noise" variance has been shown to scale cubically with power, i.e.

$$P_{NL} = a_{NL} P^3 \quad (8)$$

where a_{NL} is a power independent NLI coefficient. By using Eq. 8 in 7 and taking the inverse, for a N-span heterogeneous system [20] we get

$$\frac{1}{SNR} = \frac{1}{SNR_{TRX}} + \sum_{k=1}^N \left(\frac{NF_k \cdot h\nu (G_k - 1) B}{P_k} + a_{NLk} P_k^2 \right) \quad (9)$$

where P_k is the power at the input of span k, NF_k and G_k are the kth amplifier noise figure and gain, h is the Planck constant, ν is the light frequency and B is the signal bandwidth (e.g. equal to the symbol-rate for Nyquist signals). From Eq. 9 we note that the quantities accumulating along the line are the inverse SNRs, due to either ASE, nonlinearities or transponder imperfections.

For some common assumptions, i.e. a) ideal transponders ($P_{TRX} = 0$ and $SNR_{TRX} = +\infty$), b) identical spans and injection powers c) identical amplifiers (i.e. same noise figures) with gains compensating exactly for the signal span loss d) a supra-linear accumulation of the NLI noise along the line, Eqs. 7, and 9 yield [18]

$$SNR = \frac{P}{N \cdot NF \cdot h\nu (G - 1) B + \alpha_{NL} N^{1+\varepsilon} P^3} \quad (10)$$

where α_{NL} is a system-dependent constant that depends on the span characteristics and ε takes into account the NLI noise correlation between spans¹. a_{NL} can be then retrieved as $a_{NL} = \alpha_{NL} N^{1+\varepsilon}$.

As an example, we consider a system with N spans, operating at the optimal power P_{NLT} . The SNR is given by [18] (Eq. 14)

$$SNR_{opt} = \frac{2^{\frac{2}{3}}}{3 \cdot \alpha_{NL}^{\frac{1}{3}} N^{1+\frac{\varepsilon}{3}} [NF \cdot h\nu \cdot (G - 1) B]^{\frac{2}{3}}} \quad (11)$$

As also mentioned in [2], eq. 11 states that the optimal SNR is proportional to $\alpha_{NL}^{-\frac{1}{3}}$ or proportional to $-\frac{1}{3}\alpha_{NL}$ in a dB scale. This means e.g. that a 3 dB increase in α_{NL} would have an impact of 1 dB decrease on the SNR or directly on the Q_{BER}^2 for QPSK modulation.

In this paper, we will not discuss on the validity of the GN model however we focus on the impact of joint stochastic

¹Typical values can be found in [18] (Fig. 7) $\alpha_{NL} = 3.95 \cdot 10^{-4} mW^{-2}$ and $\varepsilon = 0.22$

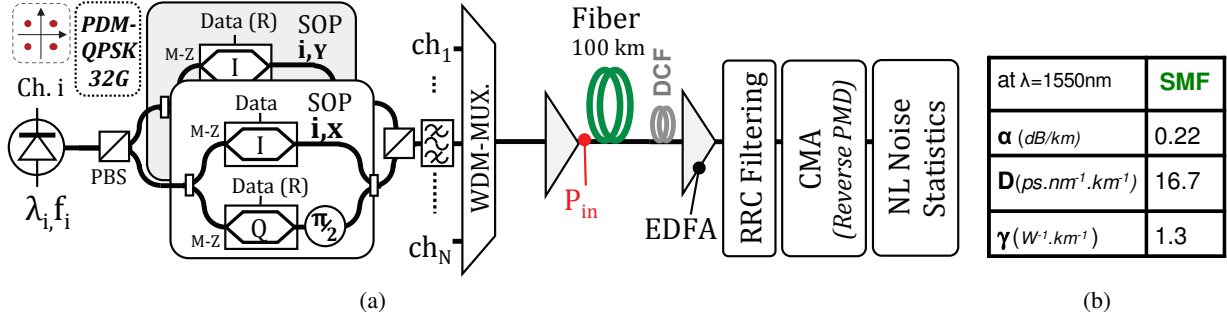


Fig. 1. Transmission system simulation setup (PBS : Polarization Beam Splitter, M-Z : Mach-Zehnder, SOP : State Of Polarization, Mux. : multiplexer, EDFA : Erbium Doped Fiber Amplifier).

PMD and Kerr effect on the variation of a_{NL} coefficient which is then practical to quickly estimate the transmission QoT and its variability.

C. Our simulation setup

In this work, we perform numerical simulations using Central and Graphics Processing Unit (CPU/GPU) computations to emulate the transmission system setup shown in Fig. 1. Our transmitter consists in a classical WDM PDM-QPSK optical transmitter multiplexing 21 channels. Each WDM channel is generated by multiplexing signals on two orthogonal polarizations that are modulated separately by In-Phase (I) and Quadrature (Q) QPSK Mach-Zehnder Modulators (MZMs) with modulation rate $R = 32$ GBauds. One PDM tributary results in an optical signal carrying 16384-long (4^7) De-Bruijn sequence generated from a Pseudo-Random Quaternary Sequence (PRQS) of symbols oversampled 128 times. All WDM channels and polarization tributaries are based on different PRQS streams. The different WDM laser signals are multiplexed following a 50 GHz frequency spacing and their Stokes's vectors are randomly drawn on the Poincaré Sphere leading to random State Of Polarizations (SOPs) for each channel. We use Root Raised Cosine (RRC) pulse shaping with a roll-off factor of 0.1.

As discussed in the previous section, we only consider a single-span transmission of 100 km fiber with launched power per channel being $P_{in} = 0$ dBm (since a_{NL} is power independent). We also assume ideal flat gain and noiseless black-box amplifiers to model Erbium Doped Fiber Amplifiers (EDFAs). As described in section II, the numerical simulation of the signal propagation along the fiber is made following either CNLSE or Manakov-PMD methods considering only loss, Group Velocity Dispersion (GVD), PMD and Kerr nonlinear effects (based on open-source Optilux simulation software [37]). Here we consider Single Mode Fiber (SMF) with nonlinear refractive index coefficient $n_2 = 2.6 \times 10^{-20} \text{ m}^2/\text{W}$ and effective area $A_{eff} = 80 \times 10^{-12} \text{ m}^2$ (nonlinear coefficient $\gamma = 1.3 \text{ W}^{-1} \cdot \text{km}^{-1}$) and with GVD coefficient $D = 16.7 \text{ ps.nm}^{-1} \cdot \text{km}^{-1}$. The SSFM step length is calculated in such a way that a maximum nonlinear phase ($\Delta\phi_{max}$) of $5 \cdot 10^{-4}$ rad is accumulated at each step. The fiber PMD modeling is performed by a concatenation of N_p birefringent plate with DGD according to the fiber PMD coefficient.

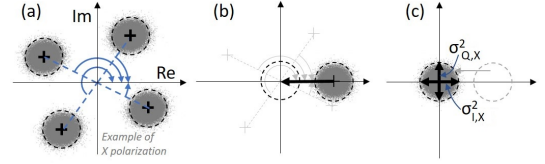


Fig. 2. a_{NL} estimation principle steps (for the central channel). (a) step 1 : finding the average complex number for each QPSK state and canceling the average state phase, (b) step 2 : canceling the real part of average superimposed QPSK states, (c) step3: I,Q-variances estimation needed for a_{NL} calculation.

At the end of the link, in order to directly estimate the NLI noise distortions, we numerically apply a full dispersion compensation (equivalent to an ideal Dispersion Compensating Fiber (DCF) as shown in Fig. 1), matched RRC filtering, ideal (data-aided) phase and polarization recovery to the signals. Here, the polarization recovery is artificially made in simulation by applying the linear reverse matrix of the whole plates concatenation (called "Reverse-PMD" block in Fig. 1). In this way the joint PMD-nonlinear distortions on signals are investigated without being altered by the coherent mixer or the equalization algorithms at the receiver side. The a_{NL} coefficient estimation is then performed on the two demultiplexed polarization tributaries of the central channel as described in the following section II-D.

D. NL noise statistic assessment parameters

The estimation of the a_{NL} coefficient is illustrated in Fig. 2. The a_{NL} coefficient is calculated through $a_{NL} = (\sigma_{I,X}^2 + \sigma_{Q,X}^2 + \sigma_{I,Y}^2 + \sigma_{Q,Y}^2) / \langle P^3 \rangle$ where P is the channel power (including both polarizations), and σ^2 stands for the variance of T -spaced sampled numerical signal ($T = 1/R$). $\sigma_{I,X}$ and $\sigma_{Q,X}$ are estimated following the principle shown in Fig. 2. Complex samples of each received QPSK state are rotated by canceling the phase and then the modulus of the state average complex number (see Fig. 2a). Then we estimate the Probability Density Function (PDF) of the gathered 16384 samples of all states (see Fig. 2c) and derive the real and imaginary variances which are equivalent to the In-Phase and Quadrature variances of the received QPSK states (see Fig. 2b).

In order to reach our objectives for estimation of the transmission performance variability caused by both PMD

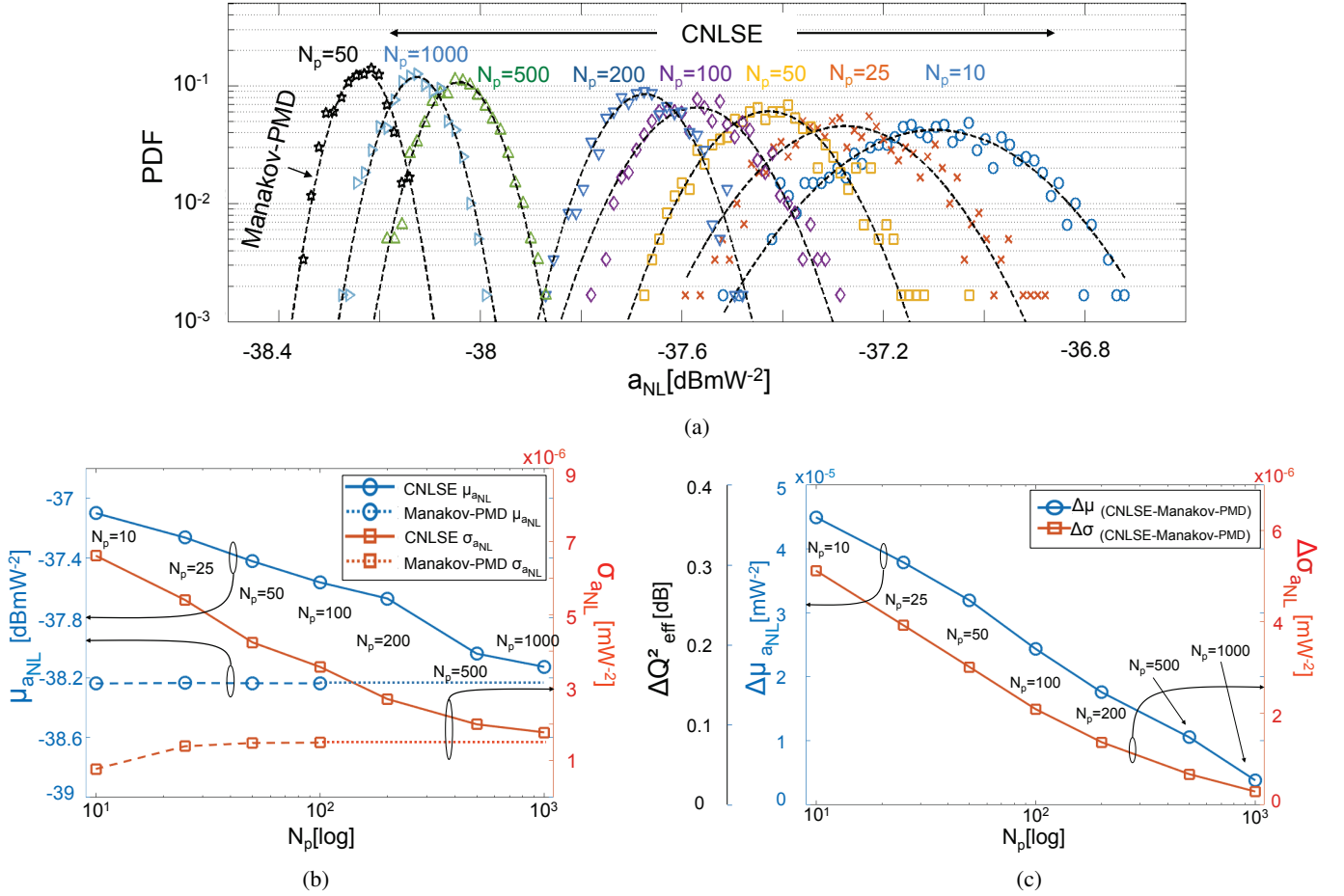


Fig. 3. (a) PDF of a_{NL} over a set of 600 transmissions with PMD coefficient of $0.13 \text{ ps}/\sqrt{\text{km}}$. (b) Boundary estimation based on N_p . (c) Estimation difference between CNLSE and Manakov-PMD methods.

and Kerr effects using CNLSE and Manakov-PMD, we then estimate a_{NL} over a set of 600 transmissions of 100km-long fiber span, each emulated with a random draw of N_p birefringent plates. This number of draws is chosen as a trade-off between a fair estimation of the Maxwellian DGD probability density function and a reasonable computation time. Finally from the PDF of this set of 600 obtained a_{NL} values, we extract the average value of a_{NL} (from values in mW^{-2}) that we will refer to as $\mu_{a_{NL}}$ (converted to dB-scale and counted in dBmW^{-2} following $10 \cdot \log_{10}[\text{mW}^{-2}]$) and its standard deviation noted as $\sigma_{a_{NL}}$ in the following.

III. COMPARISON OF CNLSE AND MANAKOV-PMD METHODS TO ESTIMATE NONLINEAR NOISE STATISTICS

A. CNLSE vs. Manakov-PMD estimation using one-span SMF transmission

Fig. 3a shows the PDF of a_{NL} over a set of 600 transmissions of 100km-long SMF span using Manakov-PMD equation with $N_p = 50$ and CNLSE with $N_p = 10, 25, 50, 100, 200, 500$ and 1000 (see section II for method descriptions). Here, we consider a PMD coefficient of $0.13 \text{ ps}/\sqrt{\text{km}}$. For all a_{NL} probability distributions markers refer to the histogram obtained from SSFM simulation results (with different N_p) while dashed curves correspond to associated Gaussian fittings.

We can observe that when the number of plates is increasing, the $\mu_{a_{NL}}$ and $\sigma_{a_{NL}}$ values obtained using CNLSE tend to decrease towards the ones obtained using Manakov-PMD method. This observation as already been shown and explained by [17] due to the fact that the impact of the nonlinear-PMD term vanishes when the birefringence correlation length tends to 0 (or equivalently N_p tends to infinite). Note that for the results using Manakov-PMD method (we recall without nonlinear-PMD term), we still observe a residual variability coming from the impact of linear stochastic PMD on Kerr nonlinear distortions. Besides our results quantify the difference of nonlinear noise statistics obtained using the two methods and depending on the actual birefringence correlation length of the considered fiber.

Manakov-PMD method with $N_p = 50$ exhibits $\mu_{a_{NL}} = -38.2 \text{ dBmW}^{-2}$ and $\sigma_{a_{NL}} = 1.5 \cdot 10^{-6} \text{ mW}^{-2}$ while, for instance, CNLSE with $N_p = 10$ and 1000 exhibits $\mu_{a_{NL}} = -37.1 \text{ dBmW}^{-2}$, $\sigma_{a_{NL}} = 6.6 \cdot 10^{-6} \text{ mW}^{-2}$ and $\mu_{a_{NL}} = -38.1 \text{ dBmW}^{-2}$, $\sigma_{a_{NL}} = 1.8 \cdot 10^{-6} \text{ mW}^{-2}$ respectively. The result show that in CNLSE simulations, the total variation of $\mu_{a_{NL}}$ is about 1.6 dB considering different N_p , while Manakov-PMD provides almost constant results changing N_p .

This observation is more accurately quantified in Fig. 3b where we report the values of $\mu_{a_{NL}}$ (left Y-axis) and $\sigma_{a_{NL}}$

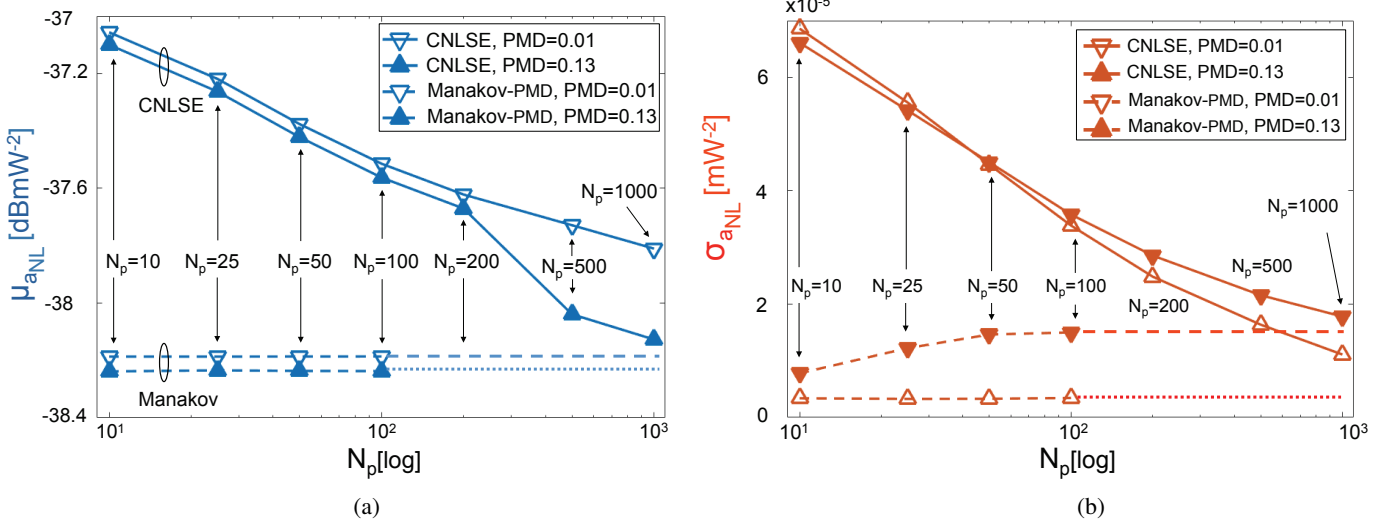


Fig. 4. μ_{aNL} (a) and σ_{aNL} (b) vs. N_p using CNSLE and Manakov-PMD methods for SMF with PMD coefficients of 0.01 and 0.13 ps/\sqrt{km} .

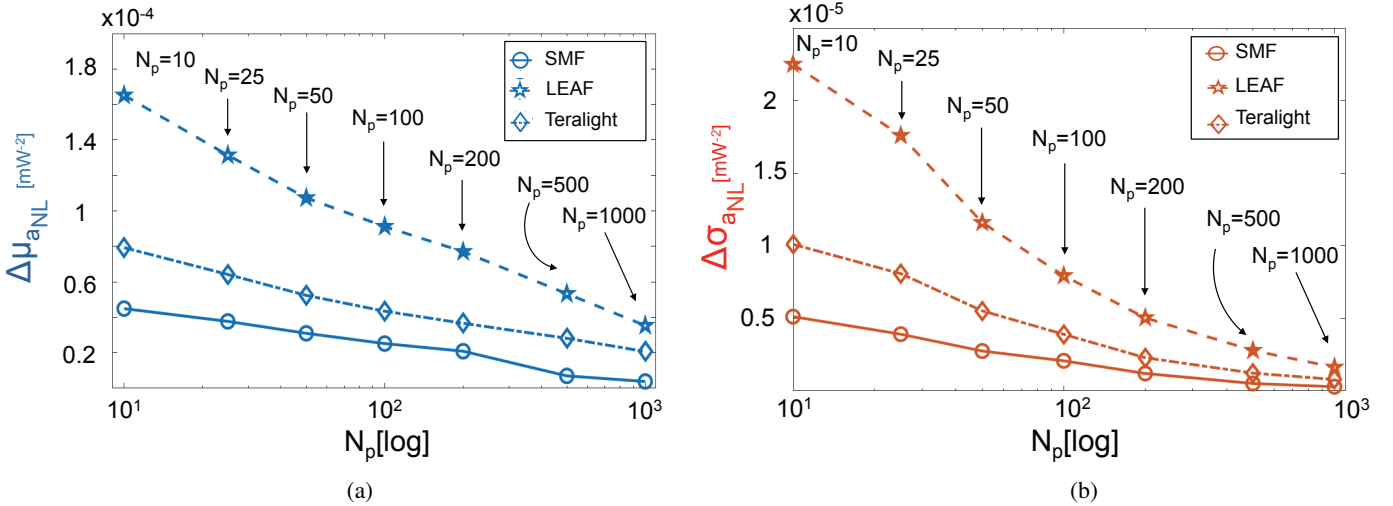


Fig. 5. $\Delta\mu_{aNL}$ (a) and $\Delta\sigma_{aNL}$ (b) vs. N_p using SMF, LEAF and Teralight fiber.

(right Y-axis) as a function of N_p in logarithmic scale for Manakov-PMD method in dashed lines and CNLSE method in solid lines. Here we can observe that Manakov-PMD method provides constant μ_{aNL} as a function of the number of plates varying from $N_p = 10$ to 100. This observation is somehow intuitive as Manakov-PMD is based on averaging Kerr nonlinearity over polarization states. Then we extrapolate the same μ_{aNL} value for higher number of plates always using Manakov-PMD method (indicated by a dotted dashed line). Besides, considering Manakov-PMD method, we equally note that the σ_{aNL} remains constant for N_p values higher than around 25 or 50 plates. Therefore we can assume that using at least $N_p = 50$ is enough to correctly estimate μ_{aNL} and σ_{aNL} in the context of Manakov-PMD modeling. For the CNLSE method, we quantify more accurately how the μ_{aNL} and σ_{aNL} values from Fig. 3a are decreasing toward the values obtained through Manakov-PMD method when N_p is increasing by plotting $\Delta\mu_{aNL} = \mu_{aNL_{CNLSE}} - \mu_{aNL_{Manakov}}$ and $\Delta\sigma_{aNL} = \sigma_{aNL_{CNLSE}} - \sigma_{aNL_{Manakov}}$ on Fig. 3c. From this results

we can discuss on two typical situations. For example, to model an hypothetical fiber having a $L_{corr.} = 2$ km, CNLSE method with $N_p = 50$ will provide more accurate results than Manakov-PMD method. However by using Manakov-PMD method μ_{aNL} and σ_{aNL} will be underestimated by 0.8 dB and $2.75 \cdot 10^{-6} mW^{-2}$ respectively, thus yielding optimistic estimations. On the other hand for a fiber having $L_{corr.} = 100$ m or less, it is better to use Manakov-PMD method with only $N_p = 50$ instead of CNLSE with $N_p = 1000$ as Manakov-PMD method provides similar results in largely less simulation time. Finally in order to rapidly estimate the $\Delta\mu_{aNL}$ and $\Delta\sigma_{aNL}$ for any N_p , we propose an empirical law for SMF by driving and exponential fitting over the results of Fig. 3c following $\Delta\mu_{aNL}(N_p) = 10^{-5} \cdot \exp(-10^{-2} \times N_p)$ and $\Delta\sigma_{aNL}(N_p) = 3.8 \cdot 10^{-6} \cdot \exp(-2 \cdot 10^{-2} \times N_p)$.

As a preliminary conclusion to this part, one can note that in order to model fibers with a lower PMD coefficient and shorter correlation length, Manakov-PMD method is relevant as being enough accurate and gaining simulation time while attempting

at $\lambda = 1550nm$	SMF	LEAF	Teralight
D ($ps \cdot nm^{-1} \cdot km^{-1}$)	16.8	4	8
γ ($W^{-1} \cdot km^{-1}$)	1.3	1.5	1.3
PMD coefficient (ps/\sqrt{km})	0.13	0.13	0.13

TABLE II
FIBER PARAMETERS

to model fibers with a higher PMD coefficient may imply the use of CNLSE method depending on the actual value of fiber L_{corr} .

B. Influence of fiber PMD coefficient

In this section we investigate the impact of the fiber PMD coefficients on the previously estimated $\mu_{a_{NL}}$ and $\sigma_{a_{NL}}$ using both CNLSE and Manakov-PMD methods. In Fig. 4a and Fig. 4b, we show the $\mu_{a_{NL}}$ and $\sigma_{a_{NL}}$ respectively as a function of N_p for both methods with two different PMD coefficients equal to $0.01 ps/\sqrt{km}$ (empty downward triangles) and $0.13 ps/\sqrt{km}$ (full upward triangles).

As the Fig. 4a shows, by increasing the N_p , the convergence of $\mu_{a_{NL}}$ obtained with CNLSE method towards the value achieved with Manakov-PMD is approximately at $N_p = 1000$ for PMD= $0.13 ps/\sqrt{km}$ (full upward triangles), while we need higher N_p values for PMD= $0.01 ps/\sqrt{km}$ (empty downward triangles). This is due to the fact that having higher PMD coefficient implies more efficient nonlinear averaging in CNLSE method and thus converge faster toward Manakov-PMD results when increasing N_p .

Moreover, as fiber DGD follows a Maxwellian distribution [38], higher PMD values provide larger DGD distribution thus the system variability due to PMD is expected to increase. This is apparent through Fig. 4b, where $\sigma_{a_{NL}}$ for PMD= $0.13 ps/\sqrt{km}$ (full upward triangles) is higher than $\sigma_{a_{NL}}$ in PMD= $0.01 ps/\sqrt{km}$ (empty downward triangles). The $\sigma_{a_{NL}}$ difference between two PMD values is not clearly visible for $N_p = 100$ considering CNLSE method. However by using Manakov-PMD method, the system variability can be more accurately evaluated for $N_p > 50$.

When decreasing the PMD coefficients the evolution of $\mu_{a_{NL}}$ and $\sigma_{a_{NL}}$ with N_p follows the same trends as the ones of Fig. 3b however we can note that the results obtained using CNLSE methods converge toward the results obtained by Manakov-PMD for larger N_p . Moreover, as the Fig. 4b shows, the difference between $\sigma_{a_{NL}}$ values obtained by Manakov-PMD or CNLSE methods is lower for higher fiber PMD coefficient values. However, when emulating a fiber with higher PMD coefficient, $\Delta\sigma_{a_{NL}}$ ($\sigma_{a_{NL}CNLSE} - \sigma_{a_{NL}Manakov}$) decreases.

C. Influence of fiber type used

In this section we investigate the difference between CNLSE and Manakov-PMD estimations by varying the fiber type. To this aim, three types of fibers are considered : aforementioned SMF, Large Effective Area Fiber (LEAF) and Teralight, with variable parameters described in Tab.II.

Fig. 5.a and Fig. 5.b show the $\Delta\mu_{a_{NL}}$ and $\Delta\sigma_{a_{NL}}$ being the differences of $\mu_{a_{NL}}$ and $\sigma_{a_{NL}}$ using either CNLSE or

Manakov-PMD methods, varying the number of plates N_p . Maximum differences are observed for LEAF then Teralight and finally SMF. Figures also indicate that LEAF requires more plates to get the same results using both methods (i.e. N_p for which $\Delta\mu_{a_{NL}} = 0$) with respect to Teralight and SMF. This is intuitive as the Kerr Length (L_{Kerr}) is lower for LEAF than for Teralight or SMF fibers and thus required shorter L_{corr} . (i.e. larger N_p) to get an averaged nonlinear effect over polarization states. It is also noticeable that $\Delta\mu_{a_{NL}}$ and $\Delta\sigma_{a_{NL}}$ are higher when using fibers with lower chromatic dispersion coefficient (particularly evident for SMF and Teralight since they have the same γ coefficient).

IV. DISCUSSION

In this section, in order to easily integrate the results in the context of optical transmission system domain, we convert the previous results obtained using a_{NL} coefficients in terms of the optimal Q^2 factor (noted Q_{opt}^2) reachable when being at the optimum launched power in the transmission fibers. Principle of this conversion is detailed in section II-B. we introduce here two quantities. Firstly δQ_{opt}^2 defined in Eq. 12 is driven from Eq.11 and corresponds to the range of variation of the optimum Q^2 factor coming from NLI noise and PMD and derived from a_{NL} variation of $\pm 3\sigma_{a_{NL}}$ around the average value $\mu_{a_{NL}}$.

$$\delta Q_{opt,CNLSE}^2(N_p) = \frac{1}{3} \cdot 10 \cdot \log_{10} \left[\frac{\mu_{a_{NL}}(N_p) + 3 \cdot \sigma_{a_{NL}}(N_p)}{\mu_{a_{NL}}(N_p) - 3 \cdot \sigma_{a_{NL}}(N_p)} \right] \quad (12)$$

Fig. 6.a shows this δQ_{opt}^2 from previous SSFM simulations using CNLSE method depending on the number of birefringent plates. The results demonstrate for instance that considering $N_p = 50$ in CNLSE method, δQ_{opt}^2 is about $0.2 dB$ for only one span SMF transmission. The mentioned Q_{opt}^2 variation range for one span LEAF and Teralight fiber is about 0.18 and $0.2 dB$ respectively considering the same simulation criteria. Increasing the N_p to 1000 plates will reduce δQ_{opt}^2 down to less than $0.1 dB$ for SMF and Teralight, while it is slightly higher for LEAF.

Secondly, we investigate the different absolute values of the Q_{opt}^2 considering CNLSE method and Manakov-PMD method. Fig. 6.b shows the difference between the $Q_{opt}^2(N_p)$ in CNLSE method and $Q_{opt}^2(50)$ in Manakov-PMD method. The figure demonstrates that a difference of $0.3 dB$ in Q_{opt}^2 between one span SSFM simulations using CNLSE and Manakov-PMD methods for $N_p = 50$.

By taking into account the quantities of Fig. 6.a and Fig. 6.b, performing numerical simulations using for instance $N_p = 50$, the maximum estimation error on the optimal Q^2 factor can be around $0.5 dB$ for just a single-span transmission.

V. CONCLUSION

Quantification and fast estimation of the QoT variability experienced by optical fiber systems are essential for the network providers in order to ensure the network reliability by having the system margin knowledge which consequently

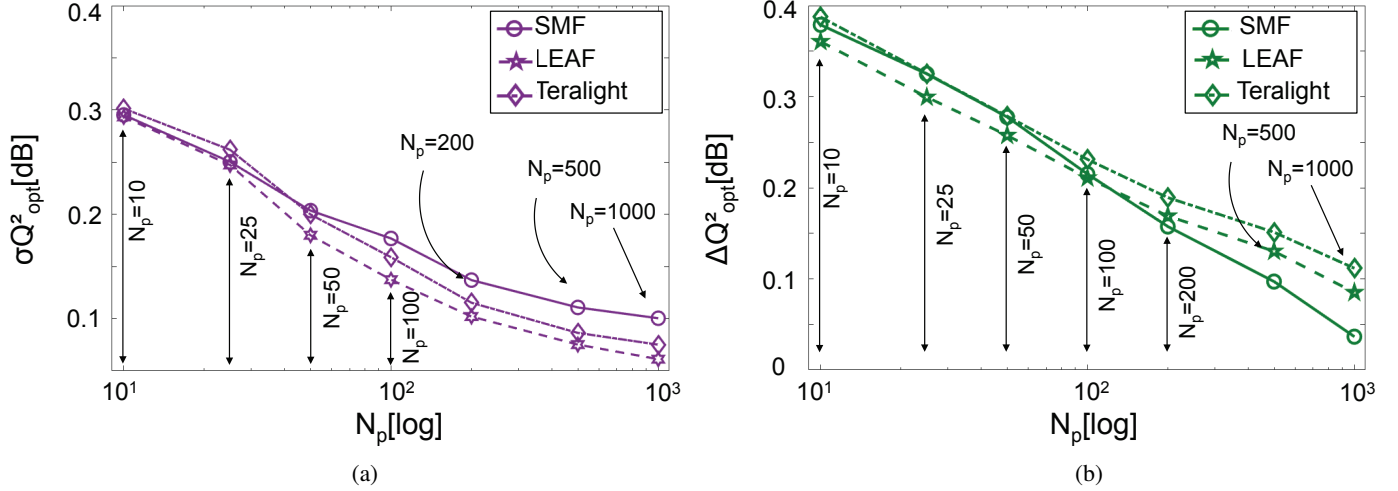


Fig. 6. (a) $\delta Q^2_{opt, CNLSE}$ and (b) $Q^2_{opt, CNLSE} - Q^2_{opt, Manakov}$ vs. N_p using SMF, LEAF and Teralight fiber.

provides cost reduction. In this work, we quantify the difference between the CNLSE and the Manakov-PMD methods in terms of QoT variability. In order to be compliant with recent fast estimation rules from GN modeling, we focus on the estimation of the NLI statistics and particularly by assessing the variability of a_{NL} that is a key parameter to deduce the QoT for all fiber launched powers and transmission distances. To this aim, we have performed a massive sets of SSFM simulation (around 46,800 simulations) to numerically estimate the a_{NL} distribution depending on the stochastic fiber birefringence concatenation using either the CNLSE or the Manakov-PMD equation.

Our results quantify the differences between the a_{NL} distributions obtained by CNLSE and Manakov-PMD methods as a function of the number of concatenation plates (N_p) used to emulate the fiber stochastic birefringence. Manakov-PMD method is shown to provide constant results for N_p higher than 50 plates. As estimating these distributions is highly time-consuming, it is then advised to perform Manakov-PMD based simulation with 50 plates, however the resulting a_{NL} distributions are accurate for the emulation of a fiber with a correlation length ($L_{corr.}$) lower than around 100 meters (or equivalently $N_p \lesssim 1000$). To accurately model fiber with $L_{corr.} \gtrsim 100m$, the CNLSE method is more accurate, nevertheless an additional time-consumption is needed to emulate the fiber birefringence with higher N_p . Moreover in this configuration, one can also perform Manakov-PMD based simulations and deduce from our results the correction to apply on the averaged a_{NL} ($\mu(a_{NL})$) or its standard deviation ($\sigma(a_{NL})$) to predict more accurate values. We also present an exponential fitting over the results in order to estimate these differences for any N_p and PMD values around $0.13 \text{ ps}/\sqrt{km}$.

Finally we have quantified the influence of the fiber type and its PMD coefficient on simulation result differences between the a_{NL} distributions obtained by either the CNLSE or the Manakov-PMD methods while N_p is increasing. Results indicates that a_{NL} distributions obtained by CNLSE converge toward the ones obtained using Manakov-PMD method for lower N_p when having a higher PMD coefficient, a lower

nonlinear coefficient γ (or equivalently a higher Kerr nonlinear length) or a higher fiber group velocity dispersion. We have shown that for higher fiber γ (i.e. LEAF), the difference of the result between the CNLSE and the Manakov-PMD is larger for any N_p with respect to SMF or Teralight fiber. For instance, we have found $\Delta\mu_{a_{NL}} = 1.3 \cdot 10^{-4} \text{ mW}^{-2}$ in the LEAF considering $N_p = 50$, while for the same simulation criteria, $\Delta\mu_{a_{NL}} = 6 \cdot 10^{-5} \text{ mW}^{-2}$ for Teralight and $\Delta\mu_{a_{NL}} = 4 \cdot 10^{-5} \text{ mW}^{-2}$ for SMF. In terms of system variability, we have found $\Delta\sigma_{a_{NL}} = 1.3 \cdot 10^{-5} \text{ mW}^{-2}$ for LEAF, while the results for Teralight and SMF are $7 \cdot 10^{-6}$ and $4 \cdot 10^{-6} \text{ mW}^{-2}$ respectively. In the end, in order to discuss the results in a simpler way, we convert the obtained variations of a_{NL} coefficient into optimal Q^2 factor variation and deduce a potential maximal estimation error of 0.5 dB while using the less suitable method among CNLSE and Manakov-PMD and considering a fiber birefringence representation by the concatenation of 50 plates.

We hope that our investigation will guide system designers to fast and accurately estimate the QoT variability of fiber optic transmission system in presence of PMD and Kerr nonlinearity.

FUNDING

The research leading to these results was partly funded by DGE (French Government) through the CELTIC+ project SENDATE-TANDEM.

ACKNOWLEDGMENTS

We want to thank Jehan Procaccia for support on computational servers, Yvan Pointurier for optical networks discussions and Pierre Sillard for giving insights on PMD fiber optics characteristics.

REFERENCES

- [1] B. A. A. Nunes, M. Mendonca, X. N. Nguyen, K. Obraczka, and T. Turetli, "A survey of software-defined networking: Past, present, and future of programmable networks," *IEEE Communications Surveys Tutorials*, vol. 16, no. 3, pp. 1617–1634, Third 2014.

- [2] P. Poggiolini, G. Bosco, A. Carena, V. Curri, Y. Jiang, and F. Forghieri, "The gn-model of fiber non-linear propagation and its applications," *Journal of Lightwave Technology*, vol. 32, no. 4, pp. 694–721, Feb 2014.
- [3] N. Rossi, A. Ghazisaeidi, and P. Ramantanis, "Stochastic nonlinear interference in dispersion managed coherent optical links," in *ECOC 2016; 42nd European Conference on Optical Communication*, Sept 2016, pp. 1–3.
- [4] S. Fazel, N. Rossi, P. Ramantanis, and Y. Frignac, "Numerical investigation and scaling rules for the estimation of nonlinear interference variability of dispersion managed and unmanaged systems in presence of pmc and kerr effects," in *ECOC 2017; 43rd European Conference on Optical Communication*, Sept 2017.
- [5] G. Keiser, *Optical fiber communications*. Wiley Online Library, 2003.
- [6] R. Ramaswami, K. Sivarajan, and G. Sasaki, *Optical networks: a practical perspective*. Morgan Kaufmann, 2009.
- [7] R.-J. Essiambre, G. Kramer, P. J. Winzer, G. J. Foschini, and B. Goebel, "Capacity limits of optical fiber networks," *Journal of Lightwave Technology*, vol. 28, no. 4, pp. 662–701, 2010.
- [8] C. R. Menyuk and B. S. Marks, "Interaction of polarization mode dispersion and nonlinearity in optical fiber transmission systems," *Journal of Lightwave Technology*, vol. 24, no. 7, pp. 2806–2826, July 2006.
- [9] O. Bertran-Pardo, J. Renaudier, G. Charlet, P. Tran, H. Mardoyan, M. Bertolini, M. Salsi, and S. Bigo, "Demonstration of the benefits brought by pmc in polarization-multiplexed systems," in *36th European Conference and Exhibition on Optical Communication*, Sept 2010, pp. 1–3.
- [10] D. Wang and C. R. Menyuk, "Polarization evolution due to the kerr non-linearity and chromatic dispersion," *Journal of Lightwave Technology*, vol. 17, no. 12, pp. 2520–2529, Dec 1999.
- [11] T. Kudou and T. Ozeki, "Nonlinear polarization-mode dispersion," in *Proceedings of Optical Fiber Communication Conference* (, Feb 1997, pp. 258–260.
- [12] M. Boroditsky, M. Bourd, and M. Tur, "Effect of nonlinearities on pmc," *Journal of Lightwave Technology*, vol. 24, no. 11, pp. 4100–4107, Nov 2006.
- [13] J. A. C. Weideman and B. M. Herbst, "Split-step methods for the solution of the nonlinear schrödinger equation," *SIAM Journal on Numerical Analysis*, vol. 23, no. 3, pp. 485–507, 1986.
- [14] G. P. Agrawal, *Nonlinear fiber optics*. Academic press, 2007.
- [15] P. Serena, N. Rossi, O. Bertran-Pardo, J. Renaudier, A. Vannucci, and A. Bononi, "Intra- versus inter-channel pmc in linearly compensated coherent pdm-psk nonlinear transmissions," *Journal of Lightwave Technology*, vol. 29, no. 11, pp. 1691–1700, June 2011.
- [16] G. Gao, X. Chen, and W. Shieh, "Influence of pmc on fiber nonlinearity compensation using digital back propagation," *Opt. Express*, vol. 20, no. 13, pp. 14406–14418, Jun 2012. [Online]. Available: <http://www.opticsexpress.org/abstract.cfm?URI=oe-20-13-14406>
- [17] D. Marcuse, C. R. Menyuk, and P. K. A. Wai, "Application of the manakov-pmc equation to studies of signal propagation in optical fibers with randomly varying birefringence," *Journal of Lightwave Technology*, vol. 15, no. 9, pp. 1735–1746, Sep 1997.
- [18] A. Bononi, N. Rossi, and P. Serena, "On the nonlinear threshold versus distance in long-haul highly-dispersive coherent systems," *Optics express*, vol. 20, no. 26, pp. B204–B216, 2012.
- [19] F. Vacondio, O. Rival, C. Simonneau, E. Grellier, A. Bononi, L. Lorcy, J.-C. Antona, and S. Bigo, "On nonlinear distortions of highly dispersive optical coherent systems," *Opt. Express*, vol. 20, no. 2, pp. 1022–1032, Jan 2012. [Online]. Available: <http://www.opticsexpress.org/abstract.cfm?URI=oe-20-2-1022>
- [20] E. Seve, P. Ramantanis, J. C. Antona, E. Grellier, O. Rival, F. Vacondio, and S. Bigo, "Semi-analytical model for the performance estimation of 100gb/s pdm-qpsk optical transmission systems without inline dispersion compensation and mixed fiber types," in *39th European Conference and Exhibition on Optical Communication (ECOC 2013)*, Sept 2013, pp. 1–3.
- [21] M. C. Jeruchim, P. Balaban, and K. S. Shanmugan, *Simulation of communication systems: modeling, methodology and techniques*. Springer Science & Business Media, 2006.
- [22] O. V. Sinkin, R. Holzlöhner, J. Zweck, and C. R. Menyuk, "Optimization of the split-step fourier method in modeling optical-fiber communications systems," *J. Lightwave Technol.*, vol. 21, no. 1, p. 61, Jan 2003. [Online]. Available: <http://jlt.osa.org/abstract.cfm?URI=jlt-21-1-61>
- [23] Q. Zhang and M. I. Hayee, "An ssf scheme to achieve comparable global simulation accuracy in wdm systems," *IEEE Photonics Technology Letters*, vol. 17, no. 9, pp. 1869–1871, Sept 2005.
- [24] A. Galtarossa, L. Palmieri, M. Schiano, and T. Tambosso, "Measurement of birefringence correlation length in long, single-mode fibers," *Opt. Lett.*, vol. 26, no. 13, pp. 962–964, Jul 2001. [Online]. Available: <http://ol.osa.org/abstract.cfm?URI=ol-26-13-962>
- [25] V. Sikka, S. Balasubramanian, A. Viswanath, and K. Srinivasan, "Correlation-based interferometric method of evaluating the beat length," *Appl. Opt.*, vol. 37, no. 2, pp. 350–351, Jan 1998. [Online]. Available: <http://ao.osa.org/abstract.cfm?URI=ao-37-2-350>
- [26] C. Antonelli, A. Mecozzi, and M. Brodsky, "Nonintrusive characterization of long-fiber-link birefringence," *Opt. Lett.*, vol. 33, no. 23, pp. 2740–2742, Dec 2008. [Online]. Available: <http://ol.osa.org/abstract.cfm?URI=ol-33-23-2740>
- [27] A. Galtarossa, L. Palmieri, M. Schiano, and T. Tambosso, "Measurement of beat length and perturbation length in long single-mode fibers by backscattered signal analysis," in *Optical Fiber Communication Conference. Technical Digest Postconference Edition. Trends in Optics and Photonics Vol.37 (IEEE Cat. No. 00CH37079)*, vol. 3, March 2000, pp. 261–263 vol.3.
- [28] —, "Statistical characterization of fiber random birefringence," *Opt. Lett.*, vol. 25, no. 18, pp. 1322–1324, Sep 2000. [Online]. Available: <http://ol.osa.org/abstract.cfm?URI=ol-25-18-1322>
- [29] —, "Measurements of beat length and perturbation length in long single-mode fibers," *Opt. Lett.*, vol. 25, no. 6, pp. 384–386, Mar 2000. [Online]. Available: <http://ol.osa.org/abstract.cfm?URI=ol-25-6-384>
- [30] A. Galtarossa, L. Palmieri, A. Pizzinat, M. Schiano, and T. Tambosso, "Measurement of local beat length and differential group delay in installed single-mode fibers," *Journal of Lightwave Technology*, vol. 18, no. 10, pp. 1389–1394, Oct 2000.
- [31] P. A. K. Wai, W. L. Kath, C. R. Menyuk, and D. Marcuse, "Nonlinear polarization mode dispersion in optical fibers with randomly varying birefringence," in *Summaries of papers presented at the Conference on Lasers and Electro-Optics*, June 1996, pp. 42–.
- [32] P. K. A. Wai, W. L. Kath, C. R. Menyuk, and J. Zhang, "Analysis of nonlinear polarization-mode dispersion in optical fibers with randomly varying birefringence," in *Proceedings of Optical Fiber Communication Conference* (, Feb 1997, pp. 257–258.
- [33] J. Proakis, *Digital Communications*. McGraw-Hill Science/Engineering/Math, August 2000, 4. [Online]. Available: <http://www.amazon.de/exec/obidos/redirect?tag=citeulike01-21&path=ASIN/0072321113>
- [34] G. P. Agrawal, *Lightwave Technology Telecommunication Systems*. John Wiley & Sons, Inc, 2005.
- [35] A. Carena, G. Bosco, V. Curri, P. Poggiolini, M. T. Taiba, and F. Forghieri, "Statistical characterization of PM-QPSK signals after propagation in uncompensated fiber links," in *Proc. 36th European Conf Optical Communication (ECOC) and Exhibition*, 2010, pp. 1–3.
- [36] E. Grellier and A. Bononi, "Quality parameter for coherent transmissions with Gaussian-distributed nonlinear noise," *Optics Express*, vol. 19, no. 13, pp. 12781–12788, Jun 2011. [Online]. Available: <http://www.opticsexpress.org/abstract.cfm?URI=oe-19-13-12781>
- [37] M. B. P. Serena and A. Vannucci. (2009) Optilux toolbox.
- [38] L. Yan, M. C. Hauer, Y. Shi, X. S. Yao, P. Ebrahimi, Y. Wang, A. E. Willner, and W. L. Kath, "Polarization-mode-dispersion emulator using variable differential-group-delay (dgd) elements and its use for experimental importance sampling," *Journal of Lightwave Technology*, vol. 22, no. 4, pp. 1051–1058, April 2004.